

# Influence of Slip of a Jeffrey Fluid Flow controlled by Peristaltic Transport with Nanoparticles in an Inclined Tube

Nemani Subadra<sup>1</sup>, Mantripragada Ananatasatya Srinivas<sup>2</sup>,  
Sunil Dutt Purohit<sup>3,\*</sup>, Sushila<sup>4</sup>

<sup>1</sup>Department of Mathematics, Geethanjali College of Engineering and Technology,  
Telangana 501301, India

<sup>2</sup>Department of Mathematics, Jawaharlal Nehru Technological University, Kukatpally, Hyderabad,  
Telangana 500085, India

<sup>3</sup>Department of HEAS (Mathematics), Rajasthan Technical University, Kota 324010, India

<sup>4</sup>Department of Physics, Vivekananda Global University, Jaipur, Rajasthan 303012, India

Received 26 August 2021; Received in revised form 15 November 2021

Accepted 04 December 2021; Available online 30 December 2021

## ABSTRACT

The present investigation mainly focused on the effect of slip on a Jeffrey fluid flow with nanoparticles in an inclined tube. Homotopy perturbation method is used to find the expressions for temperature and concentration. Analytical expressions for axial velocity, pressure drop, heat and mass transfer phenomena were calculated. The nature of these variables was interpreted by using the graphs for various pertinent parameters. Stream line patterns were depicted at the end. The flow velocity can be controlled by increasing/decreasing the parameters  $N_b, N_t, G_r, B_r, \lambda_1$ .

**Keywords:** Homotopy perturbation method; Jeffrey fluid; Prone tube; Slip effect

## 1. Introduction

Many researchers have recently focused on non-Newtonian fluid models due to their ubiquitous use in engineering and industry to investigate the thermo-physical characteristics of various parameters to improve the heat transmission properties of these liquids. Several investigators researched diverse non-Newtonian model fluids, Jeffrey fluid being one of them, for

the exploration of various rheological characteristics. Shapiro et al., [16], Chu and Fang [2], Maruthi Prasad and Radhakrishnamacharya, [9], Prasad et al. [14], Subadra et al. [11].

Researchers are paying close attention to nanotechnology these days because of its applicability in health and industrial domains. S.U.S. Choi [15] was a pioneer in the field of nanotechnology

research. Eastman et al. [3] shown that by adding nanoparticles to the base fluids, the thermal conductivity of the base fluids may be increased by 60%. Many other researchers have also worked in this topic. Significant contributions to this field of study have been made by Prasad et al. [8], Ellahi [4], Agarwal et al. [1], Jamshed et al. [7], Subadra et al. [8] and W. Jamshed et al. [17].

The majority of the researchers conducted their investigation with no slip boundary conditions at the vessel walls. Blood vessel walls, on the other hand, may be mobile, flexible, and porous in nature. Peristaltic transfer in a slip flow was studied by Chu and Fang [2]. Naby and Shamy investigated the effects of slip on the peristaltic transport of a power-law fluid via an inclined tube [12]. Slip effects on peristaltic transport in an inclined channel with mass transfer and chemical reaction were investigated by Hayat et al. [5]. Prasad et al. [8] investigated research on effect of slip of nanofluid in an inclined tube.

This work examines the peristaltic motion of nanoparticles submerged in Jeffery fluid in a conduit, as well as the impacts of heat and mass transmission. For axial velocity, pressure drop, frictional force, heat, and mass transfer effects, analytical formulas have been computed and graphed. The patterns of stream lines and trapped bolus have been illustrated.

**Nomenclature**

- $a^*$  Radius of uniform cross section,
- $b^*$  Wave amplitude,
- $c^*$  Speed of the wave,
- $N_b$  Brownian Motion Parameter,
- $N_t$  Thermophoresis Parameter,
- $p$  Pressure in wave,
- $P$  Pressure in fixed frame,
- $B_r$  Local Nanoparticle Grashof Number,
- $G_r$  Local Temperature Grashof Number,
- $F$  Frictional Force,

- $r$  Radial coordinate,
- $t$  Time,
- $k$  Permeability Constant,
- $U, W$  Velocity components in the laboratory frame,
- $u, w$  Velocity components in the wave frame.

**Greek Symbols**

- $\mu$  Coefficient of viscosity,
- $\lambda^*$  Wavelength,
- $\tau$  Cauchy stress tensor,
- $\lambda_1$  Ratio of relaxation to retardation times,
- $\lambda_2$  Retardation time,
- $\gamma$  Shear rate,
- $\theta_1$  Temperature,
- $\sigma_1$  Concentration,
- $\alpha$  Inclined angle.

**2. Mathematical Formulation**

In an inclined tube, a two-dimensional peristaltic propulsion of an incompressible Jeffrey model with permeable walls is investigated.

By using the cylindrical polar coordinate system  $(R, \theta, Z)$ , the fluid motion is caused by a sinusoidal wave train is

$$R = H(z, t) = a^* + b^* \sin \frac{2\pi}{\lambda^*} (Z - c^* t). \tag{2.1}$$

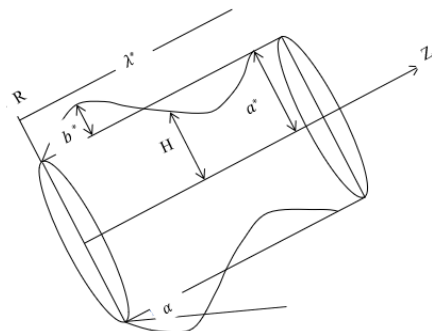


**Fig.1.** Geometry of the Problem.

For the Jeffrey model, the equation regulating the additional stress tensor  $\tau$  is

$$\tau = \frac{\mu}{1 + \lambda_1} \left( \frac{dY}{dt} + \lambda_2 \frac{d^2Y}{dt^2} \right). \tag{2.2}$$

To shift to wave frame, perform the transformations listed below.

$$z = Z - c^*t, r = R, \theta = \Theta, w = W - c^*r, u = U. \tag{2.3}$$

The equations of the Jeffery fluid flow (Nadeem et al. [13]) with nanoparticles may be obtained by using non-dimensionalization plus lubrication theory approximations:

$$\frac{\partial p}{\partial r} = 0, \tag{2.4}$$

$$\frac{1}{1 + \lambda_1} \frac{1}{r} \frac{\partial}{\partial r} \left( r \frac{\partial w}{\partial r} \right) = -\frac{\partial p}{\partial z} + G_r \theta_1 + B_r \sigma_1 + \frac{\sin \alpha}{F}, \tag{2.5}$$

$$0 = \frac{1}{r} \frac{\partial}{\partial r} \left( r \frac{\partial \theta_1}{\partial r} \right) + N_b \frac{\partial \sigma_1}{\partial r} \frac{\partial \theta_1}{\partial r} + N_t \left( \frac{\partial \theta_1}{\partial r} \right), \tag{2.6}$$

$$0 = \frac{1}{r} \frac{\partial}{\partial r} \left( r \frac{\partial \sigma_1}{\partial r} \right) + \left( \frac{N_t}{N_b} \right) \frac{1}{r} \frac{\partial}{\partial r} \left( r \frac{\partial \theta_1}{\partial r} \right), \tag{2.7}$$

The following are the boundary conditions:

$$\frac{\partial w}{\partial r} = 0, \frac{\partial \theta_1}{\partial r} = 0 \text{ and } \frac{\partial \sigma_1}{\partial r} = 0 \text{ at } r = 0, \tag{2.8}$$

$$w = -k \frac{\partial w}{\partial r} = 0, \theta_1 = 0, \sigma_1 = 0 \text{ at } r = h. \tag{2.9}$$

### 3. Problem-Solving Approach

He's [6] HPM is used to get approximate solutions for  $\theta_1$  and  $\sigma_1$  in Eq. (2.6) and Eq. (2.7). The expressions for  $\theta_1$  and  $\sigma_1$  are obtained by applying boundary

conditions and assuming the initial approximations of

$$\theta_{10}(r, z) = \frac{r^2 - h^2}{4} \text{ and } \sigma_{10}(r, z) = -\left( \frac{r^2 - h^2}{4} \right),$$

$$\theta_1 = (N_b - N_t)(N_b - 2N_t) \left( \frac{r^6 - h^6}{1152} \right) - (N_b - 2N_t) \left( \frac{r^4 - h^4}{64} \right), \tag{3.1}$$

$$\sigma_1 = -\left( \frac{N_t}{N_b} \right) (N_b - N_t) \left( \frac{r^4 - h^4}{64} \right). \tag{3.2}$$

Substituting Eq. (3.1) and Eq. (3.2) in Eq. (2.5) and applying boundary conditions Eq. (2.8) and Eq. (2.9), the expression for  $w$  is

$$w = -(1 + \lambda_1) \frac{dp}{dz} \left( \frac{r^2}{4} - \frac{h^2}{4} - \frac{kh}{2} \right) + (1 + \lambda_1) \frac{\sin \alpha}{F} \left( \frac{r^2}{4} - \frac{h^2}{4} - \frac{kh}{2} \right) + \frac{G_r}{1152} (1 + \lambda_1) (N_b - N_t) (N_b - 2N_t) \left( \frac{r^8}{64} - \frac{r^2 h^6}{4} + \frac{15h^8}{64} + \frac{3kh^7}{8} \right) - \frac{G_r}{64} (1 + \lambda_1) (N_b - 2N_t) \left( \frac{r^6}{36} - \frac{r^2 h^4}{4} + \frac{2h^6}{9} + \frac{kh^5}{3} \right) - \frac{B_r}{64} (1 + \lambda_1) \left( \frac{N_t}{N_b} \right) (N_b - 2N_t) \left( \frac{r^6}{36} - \frac{r^2 h^4}{4} + \frac{2h^6}{9} + \frac{kh^5}{3} \right). \tag{3.3}$$

In the moving frame, the dimensionless flux  $q$  is given by

$$q = \int_0^h 2rw \, dr. \tag{3.4}$$

The pressure drops over a wave length  $\Delta p_\lambda$  is calculated as follows:

$$\Delta p_\lambda = -\int_0^1 \frac{dp}{dz} \, dz. \tag{3.5}$$

The expression for  $\Delta p_\lambda$  is as follows

$$\Delta p_\lambda = qL_1 + L_2, \tag{3.6}$$

where

$$L_1 = -\frac{1}{1 + \lambda_1} \int_0^1 \frac{1}{A} \, dz,$$

$$L_2 = -\frac{\sin \alpha}{F} + \frac{G_r}{576}(N_b - N_t)(N_b - 2N_t) \int_0^1 \frac{B}{A} dz - \frac{G_r}{32}(N_b - 2N_t) \int_0^1 \frac{C}{A} dz - \frac{B_r}{32} \left( \frac{N_t}{N_b} \right) (N_b - 2N_t) \int_0^1 \frac{C}{A} dz,$$

where,

$$A = \frac{h^4}{8} + \frac{kh^3}{2},$$

$$B = \frac{9h^{10}}{160} + \frac{3kh^9}{16},$$

$$C = \frac{5h^8}{96} + \frac{kh^7}{6}.$$

Using the same approach as Shapiro et al. [16], Over a period of time, the average time flux given by the laboratory frame was

$$\bar{Q} = 1 + \frac{\varepsilon^2}{2} + q. \tag{3.7}$$

At the tube wall the dimensional less frictional force  $\bar{F}$  is

$$\bar{F} = \int_0^1 h^2 \left( -\frac{dp}{dz} \right) dz. \tag{3.8}$$

The heat transfer coefficient and mass transfer coefficient at the tube wall are:

$$Z_\theta(r, z) = \left( \frac{\partial h}{\partial z} \right) \left( \frac{\partial \theta_1}{\partial r} \right)$$

and

$$Z_\sigma(r, z) = \left( \frac{\partial h}{\partial z} \right) \left( \frac{\partial \sigma_1}{\partial r} \right). \tag{3.9}$$

### 4. Findings and Discussions

The graphs depicting axial velocity, pressure drop, frictional force, heat transfer pressure drop, and mass transfer coefficient were developed using Mathematica 11.0 software.

#### 4.1 Pressure Drop

Figs. 1-7 plots the pressure drop versus time averaged flux for various values of flow parameters. It is observed that,

increasing in  $N_b, \lambda_1, \alpha$ , there is a negative impact in pressure drop. This has therapeutic implications since sustaining larger pressure gradients, which has a demonstrable influence in the drug delivery system, has implications.  $\Delta p_\lambda$  increases for greater magnitude of thermophoresis  $N_t, G_r, B_r$  and  $k$ .

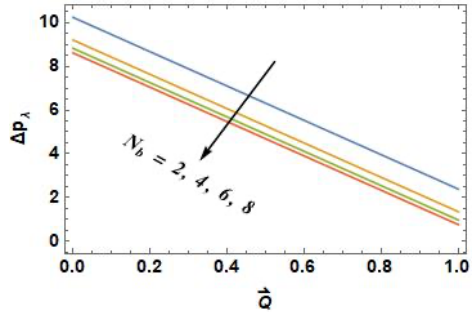


Fig. 1. Fluctuations in Pressure Drop for  $N_b$ .

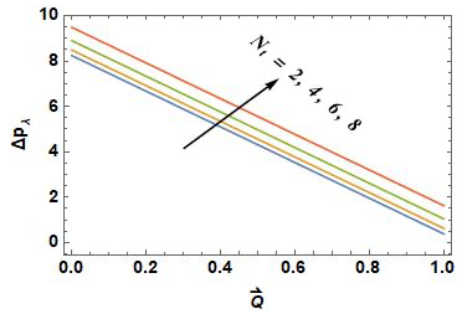


Fig. 2. Fluctuations in Pressure Drop for  $N_t$ .

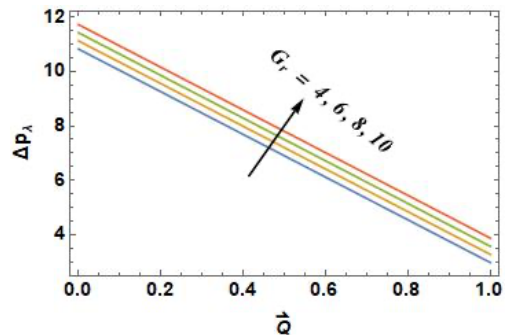


Fig. 3. Fluctuations in Pressure Drop for  $G_r$ .

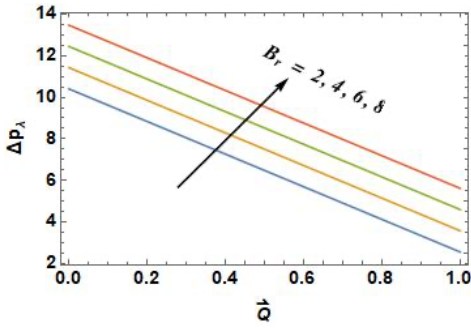


Fig. 4. Fluctuations in Pressure Drop for  $B_r$ .

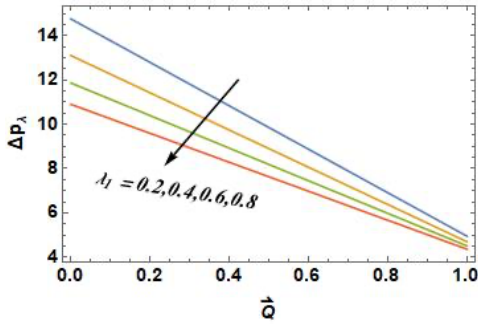


Fig. 5. Fluctuations in Pressure Drop for  $\lambda_1$ .

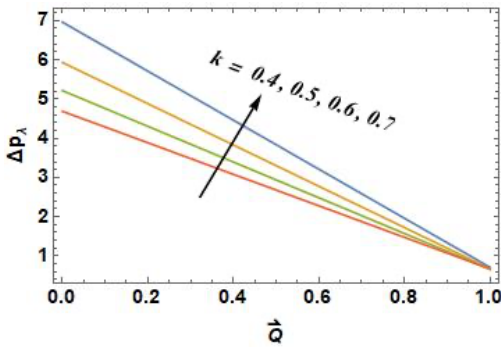


Fig. 6. Fluctuations in Pressure Drop for  $k$ .

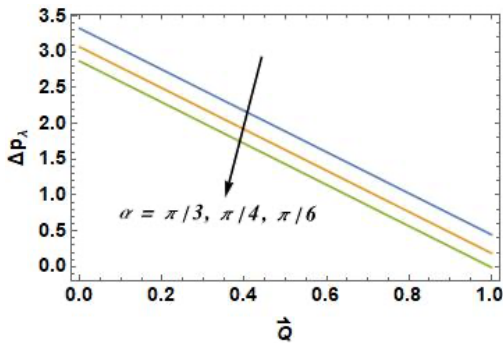


Fig. 7. Fluctuations in Pressure Drop for  $\alpha$ .

#### 4.2 Frictional force

It is apparent that, frictional forces  $\bar{F}$  is upsurged by growing  $N_t, G_r, B_r, \alpha$ .

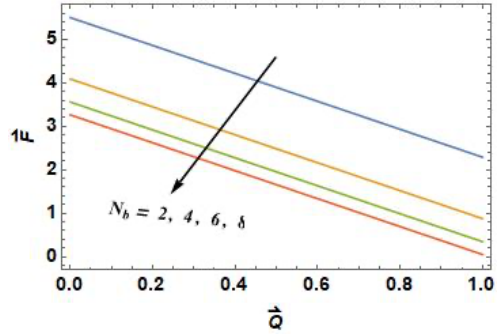


Fig. 8. Fluctuations in Frictional Force for  $N_b$ .

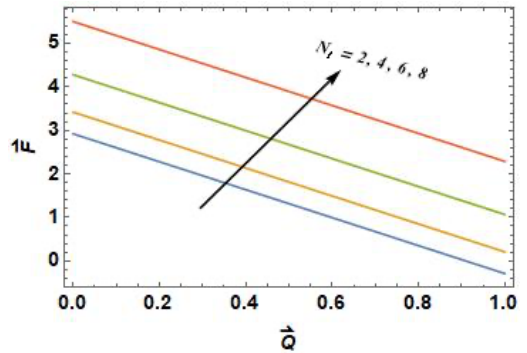


Fig. 9. Fluctuations in Frictional Force for  $N_t$ .

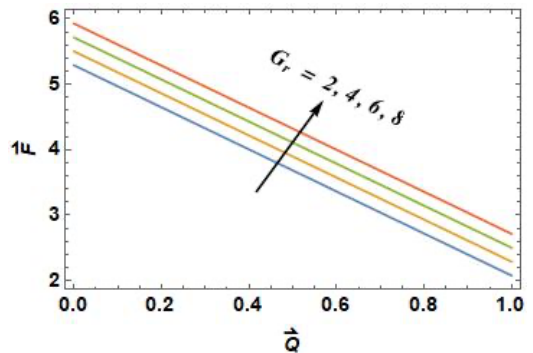


Fig. 10. Fluctuations in Frictional Force for  $G_r$ .

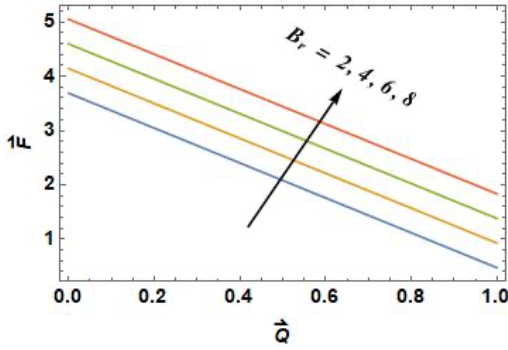


Fig. 11. Fluctuations in Frictional Force for  $B_r$ .

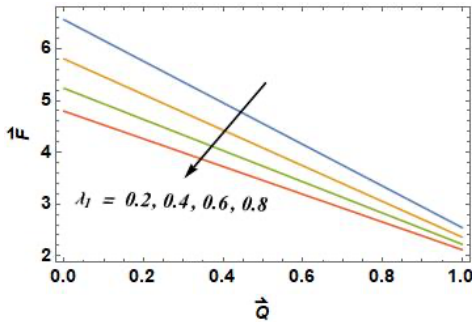


Fig. 12. Fluctuations in Frictional Force for  $\lambda_1$ .

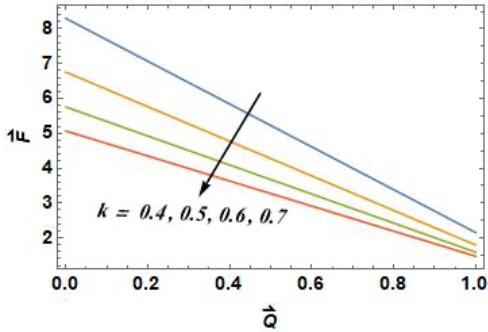


Fig. 13. Fluctuations in Frictional Force for  $k$ .

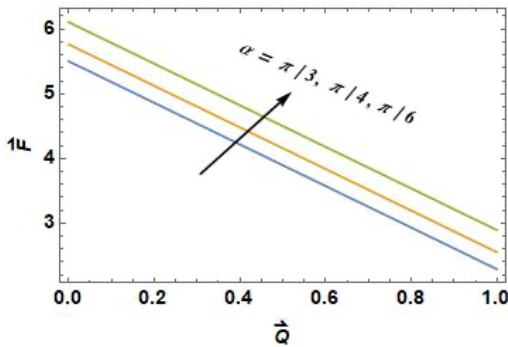


Fig. 14. Fluctuations in Frictional Force for  $\alpha$ .

4.3 Temperature

Significant raise in temperature is sustained as the upsurges in Brownian motion ( $N_b$ ) and an opposite behaviour is found with thermophoresis.

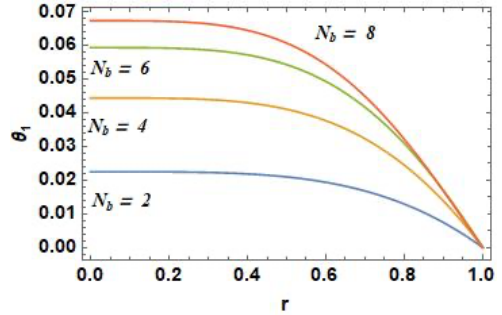


Fig. 15. Effect of  $N_b$  on Temperature.

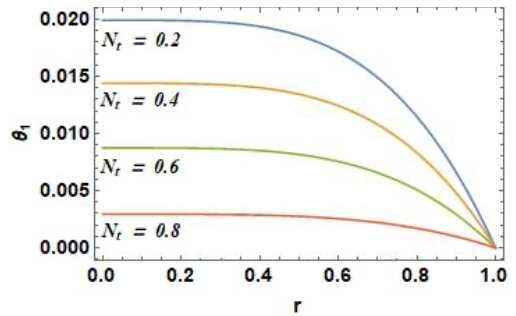


Fig. 16. Effect of  $N_t$  on Temperature.

4.4 Concentration

It can be seen from the graph that concentration increases as  $N_t$  increases. It may be deduced that a constant increase in the firmness of thermophoretic effects results in a larger mass flow as temperature rises, increasing the concentration.

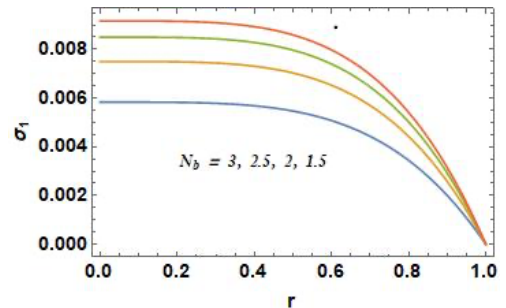


Fig. 17. Effect of  $N_b$  on Concentration.

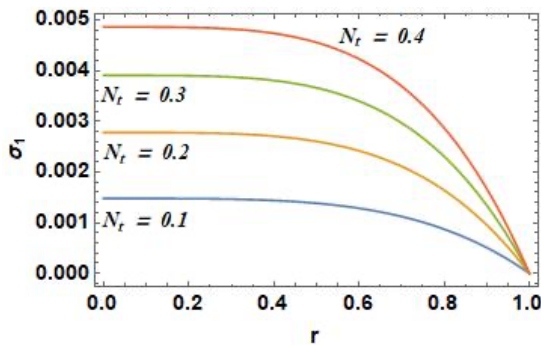


Fig. 18. Effect of  $N_t$  on Concentration.

#### 4.5 Heat Transfer Coefficient

It is interesting to observe that, absolute value of coefficient of heat transfer is increasing for  $N_b$  and decreasing for  $N_t$ .

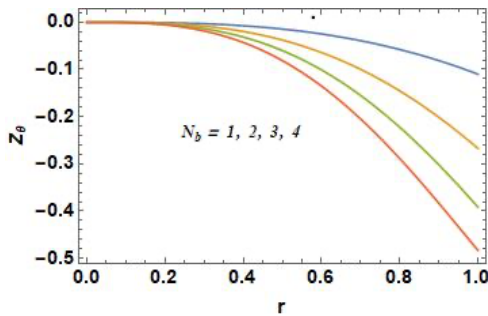


Fig. 19. Impact of  $N_b$  on Heat Transfer Coefficient.

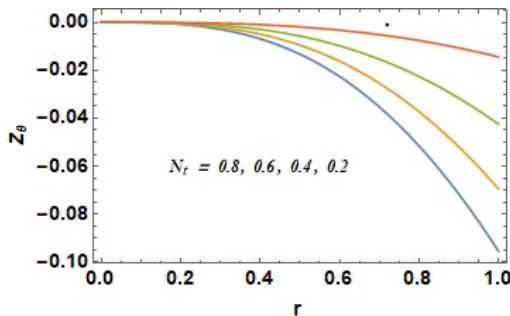


Fig. 20. Impact of  $N_t$  on Heat Transfer Coefficient.

#### 4.6 Mass Transfer Coefficient

It is observed that, absolute value of coefficient of mass transfer is increasing for  $N_b$  and decreasing for  $N_t$ .

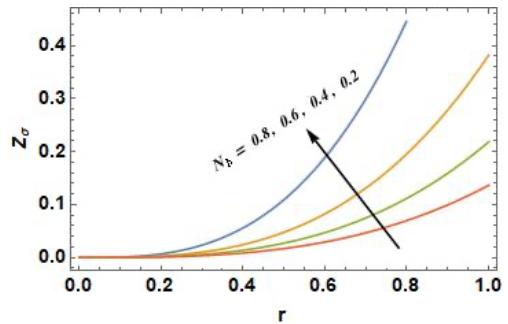


Fig. 21. Impact of  $N_b$  on Mass Transfer Coefficient.

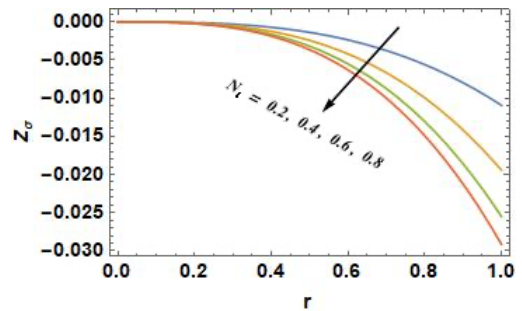
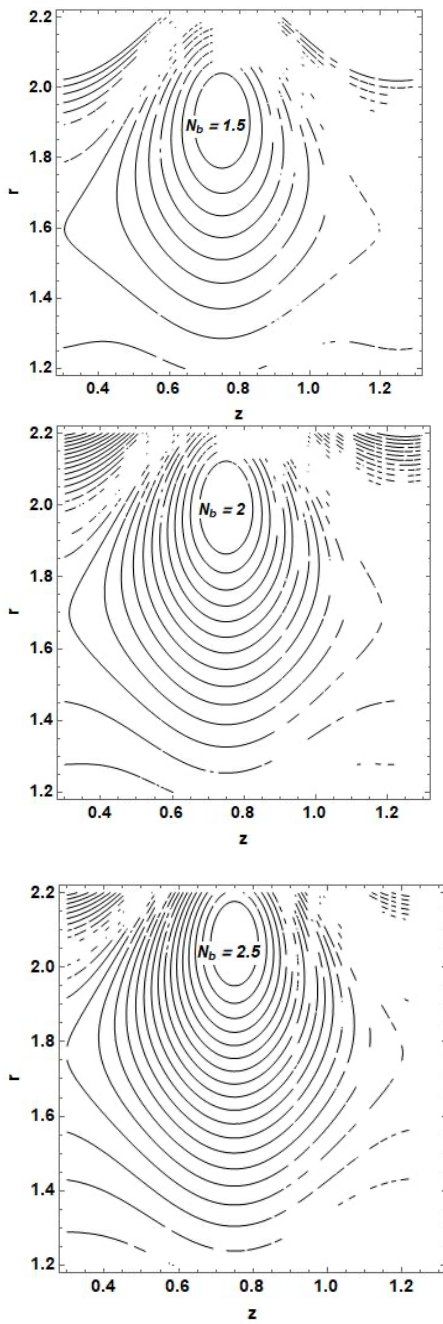


Fig. 22. Impact of  $N_t$  on Mass Transfer Coefficient.

#### 4.7 Trapping

In peristaltic motion, the trapping phenomena is much more thought-provoking. The following figures shows that, the size of the trapped bolus increases with the increases of parameters. So physically the velocity can be controlled by increasing/decreasing these pertinent parameters.



**Fig. 23.** Streamlines for different values of  $N_b$ .

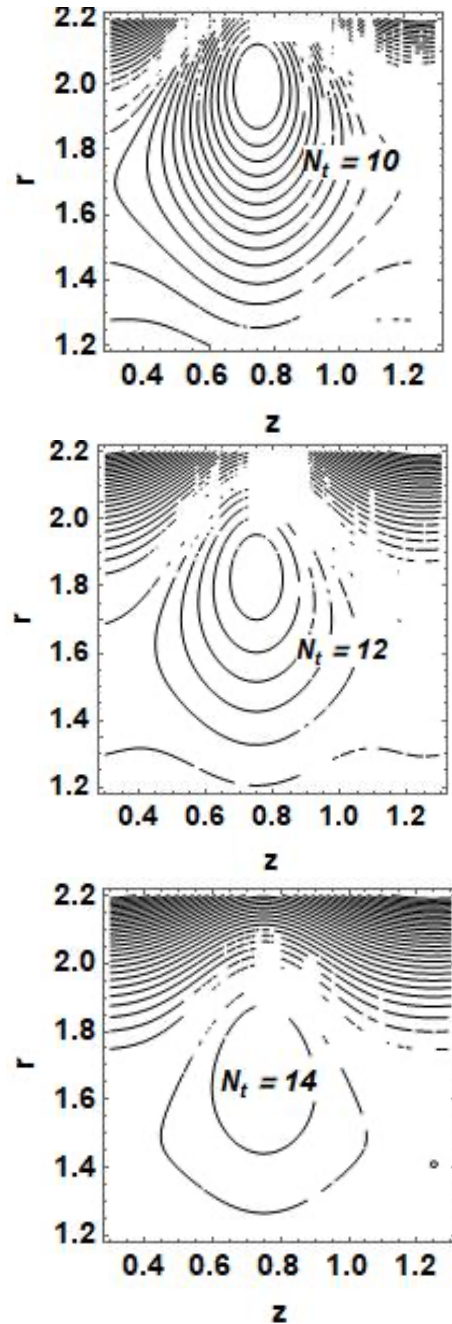


**Fig. 24.** Streamlines for different values of  $N_t$ .

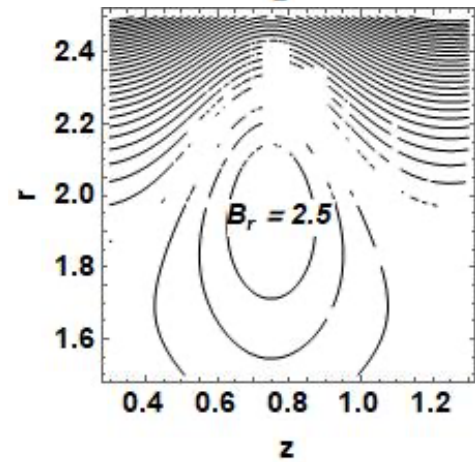
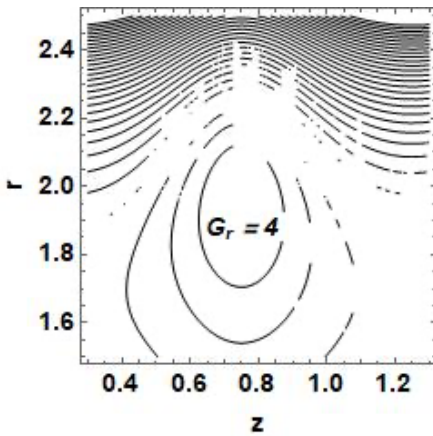
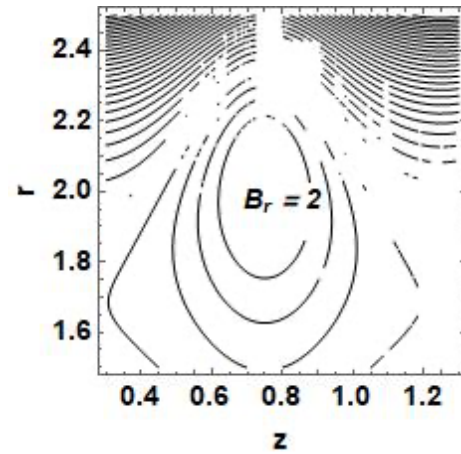
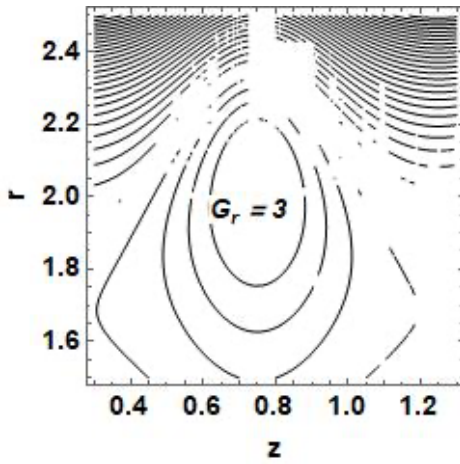
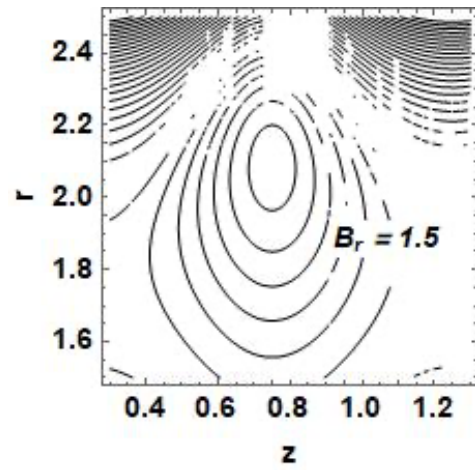
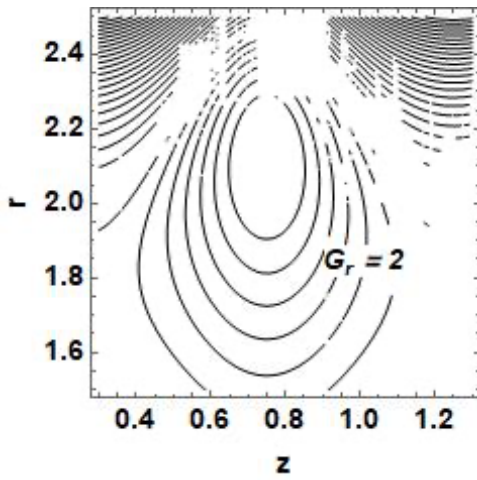


Fig. 25. Streamlines for different values of  $G_r$ .

Fig. 26. Streamlines for different values of  $B_r$ .

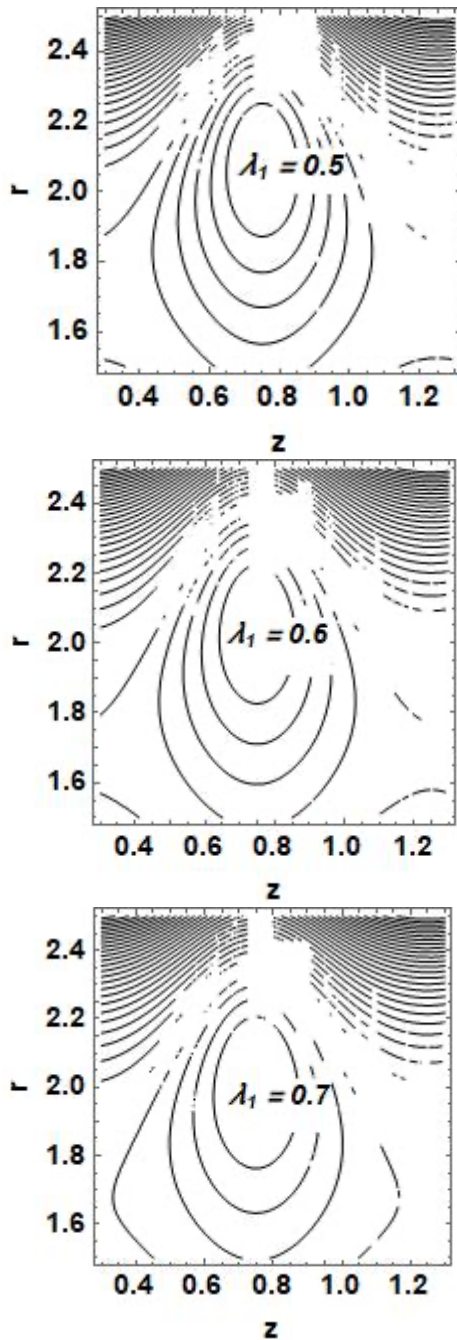


Fig. 27. Streamlines for different values of  $\lambda_1$ .

The results of this paper are coinciding with results of the paper of Subhadra et al. if no slip boundary condition is used in a straight tube.

## 5. Conclusion

- (i) The major conclusions of this investigations are
- (ii) If there is an increase in  $N_b, \lambda_1, \alpha$ , there is a negative impact on pressure drop.
- (iii) Frictional force  $\bar{F}$  is upsurged by growing  $N_t, G_r, B_r, \alpha$ .
- (iv) Significant raise in temperature is sustained as the upsurges in Brownian motion ( $N_b$ ) and an opposite behaviour is found with thermophoresis.
- (v) Concentration increases as  $N_t$  increases. It may be deduced that a constant increase in the firmness of thermophoretic effects results in a larger mass flow as temperature rises, increasing the concentration.
- (vi) Absolute value of coefficient of heat transfer is increasing for  $N_b$  and decreasing for  $N_t$ .
- (vii) Absolute value of coefficient of mass transfer is increasing for  $N_b$  and decreasing for  $N_t$ .
- (viii) The size of the trapped bolus increases with the increases of parameters. So physically the velocity can be controlled by increasing/decreasing these pertinent parameters.

## References

- [1] Shapiro, A.H., Jaffrin, M.Y., Weinberg, S.L., (1969). Peristaltic pumping with long wavelengths at low Reynolds number. *J. Fluid Mech.* 37, 799-825.
- [2] Chu, W.K.-H., Fang, J., (2000). Peristaltic transport in a slip flow. *Eur. Phys. J. B- Condens. Matter Complex Syst.* 16, 543-7.
- [3] Maruthi Prasad, K., Radhakrishnamacharya, G., (2008). Flow of Herschel-Bulkley fluid through an inclined tube of non-uniform cross-

- section with multiple stenoses. *Arch. Mech.* 60, 161-72.
- [4] Prasad, K.M., Subadra, N., Srinivas, M., (2017). Thermal Effects of Two Immiscible Fluids in a Circular Tube with Nano Particles. *J. Nanofluids* 6, 105-19.
- [5] N. Subadra, M. A. Srinivas, and Sunil Dutt Purohit, (2020). Mathematical approach to study heat and mass transfer effects in transport phenomena of a non-Newtonian fluid, *AIP Conference Proceedings* 2269, 060006.
- [6] S. U.S. Choi, J.A.E., (1995). Enhancing thermal conductivity of fluids with nanoparticles. *ASME FED. Proc. ASME Int. Mech. Eng. Congr. Expo.* 66. <https://doi.org/10.3390/app8020192>
- [7] Eastman, J., Choi, U., Li, S., Thompson, L., Lee, S., (1996). Enhanced thermal conductivity through the development of nanofluids. Presented at the MRS proceedings, Cambridge Univ Press, p. 3.
- [8] K Maruthi Prasad, N Subadra. (2019). Influence of Slip-on Peristaltic Motion of a Nanofluid Prone to the Tube, *Numerical Heat Transfer and Fluid Flow*, 519-26.
- [9] Ellahi, R., (2018). Special Issue on Recent Developments of Nanofluids. *Appl. Sci.* 8, 192.
- [10] Agrawal, P., Dadheech, P. K., Jat, R. N., Nisar, K. S., Bohra, M., & Purohit, S. D., (2021). Magneto Marangoni flow of  $\gamma$ -AL<sub>2</sub>O<sub>3</sub> nanofluids with thermal radiation and heat source/sink effects over a stretching surface embedded in porous medium. *Case Studies in Thermal Engineering*, 23, 100802., <https://doi.org/10.1016/j.csite.2020.100802>
- [11] Jamshed, W., Nasir, N.A.A.M., Isa, S.S.P.M. et al., (2021). Thermal Growth in Solar Water Pump using Prandtl–Eyring Hybrid Nanofluid: A Solar Energy Application. *Scientific Reports*, 11, 18704. <https://doi.org/10.1038/s41598-021-98103-8>
- [12] W. Jamshed, Kottakkaran Sooppy Nisar, (2021). Computational Single Phase Comparative Study of Williamson Nanofluid in Parabolic Trough Solar Collector Via Keller box Method, *International Journal of Energy Research*, <https://doi.org/10.1002/er.6554>
- [13] Naby, A. E. H. A. El, & Shamy, I. El. (2007). Slip effects on peristaltic transport of power-law fluid through an inclined tube. *Applied Mathematical Sciences*, 1(60), 2967-80.
- [14] Hayat, T., Abbasi, F. M., Ahmad, B., & Alsaedi, A. (2014). Peristaltic transport of Carreau-Yasuda fluid in a curved channel with slip effects. *PloS One*, 9(4), e95070.
- [15] Nadeem, S., Riaz, A., Ellahi, R., Akbar, N.S., (2014). Mathematical model for the peristaltic flow of Jeffrey fluid with nanoparticles phenomenon through a rectangular duct. *Appl. Nanosci.* 4, 613–624. <https://doi.org/10.1007/s13204-013-0238-5>
- [16] He JH. (1999). Homotopy Perturbation Technique. *Comput. Methods Appl. Mech. Eng.* 178, 257-62.
- [17] N Subadra, K Maruthi Prasad, S Ravi Prasad Rao, (2020), Influence of Slip and Heat and Mass Transfer Effects on Peristaltic motion of Power-law fluid Prone to the Tube, *Journal of Physics: Conference Series*, 1495(1), 012039.